

## Ultrafast recombination and trapping in amorphous silicon

A. Esser, K. Seibert, and H. Kurz

*Institut für Halbleitertechnik, Rheinisch-Westfälische Technische Hochschule Aachen,  
D-5100 Aachen, Federal Republic of Germany*

G. N. Parsons, C. Wang, B. N. Davidson, G. Lucovsky, and R. J. Nemanich

*Department of Physics and Department of Materials Science and Engineering, North Carolina State University,  
Raleigh, North Carolina 27695-8202*

(Received 23 August 1989)

We have studied the time-resolved reflectivity and transmission changes induced by femtosecond laser pulses in hydrogenated and nonhydrogenated amorphous silicon thin films, *a*-Si:H and *a*-Si, respectively. By varying the pump power, and hence the photoexcited free-carrier densities, by several orders of magnitude, a quadratic, nonradiative recombination process has been identified that controls the density of free carriers on a picosecond time scale for excitation levels above  $5 \times 10^{18} \text{ cm}^{-3}$  in *a*-Si:H and above  $5 \times 10^{19} \text{ cm}^{-3}$  in *a*-Si. At lower free-carrier densities, the reflectivity transients display the dynamics expected from a trapping mechanism. We suggest that the process that dominates for the higher free-carrier densities may result from Auger recombination but with a dependence on the carrier density that is different from that which has been observed in crystalline semiconductors where *k* selection prevails.

### I. INTRODUCTION

The relaxation of optically excited carriers in hydrogenated amorphous silicon (*a*-Si:H) has been the subject of recent time-resolved optical investigations on picosecond and subpicosecond time scales.<sup>1-6</sup> The results to date, relative to the recovery of induced absorption and reflection changes on a picosecond time scale,<sup>1-6</sup> have been explained on the basis of multiple trapping within band-tail states of the amorphous material. Multiple trapping implies that the dynamics of the recovery of the induced optical changes depend only on the density of localized band-tail and defect states, and not of the density of the optically generated free carriers. Subpicosecond transients studied via absorption, however, show that the recovery dynamics can, under conditions of high pulse power, depend on the density of optically generated carriers.<sup>3</sup> This density dependence of the recombination dynamics has been explained by a transition from multiple trapping at low densities to direct trapping at high densities, where the photogenerated free carriers are assumed to relax directly from extended states to deep band-tail states.<sup>3</sup>

These particular interpretations of picosecond and subpicosecond optical relaxation mechanisms rely heavily on assumptions concerning the optical response of trapped carriers. Specifically, as the carriers become trapped in deeper states, their contributions to the induced changes in the absorption and reflection are assumed to decrease. In this particular model, recombination of carriers is not significant on a picosecond time scale, but only becomes important on a nanosecond or longer time scales.<sup>2</sup> In contrast, an ultrafast, bimolecular nonradiative recombination process has been invoked to explain the results of photoluminescence experiments at high excitation lev-

els ( $> 2 \times 10^{18} \text{ cm}^{-3}$ ).<sup>7,8</sup> Street *et al.*<sup>8</sup> have suggested that this is an Auger process; however, Rehm and Fischer<sup>7</sup> have found that at high excitation levels, the recombination rate exhibits a quadratic rather than a cubic dependence on optically injected free-carrier density *N*. This deviation from an expected  $N^3$  dependence for an Auger process has been attributed to a high density of spatially overlapping electron-hole (*e-h*) pairs.<sup>7</sup> In this paper, we explore ultrafast recombination processes at high optical-generation levels by studying the time-resolved changes in the optical reflectivity. The results indicate a transition between an ultrafast recombination process at high-excitation levels, and a free-carrier trapping mechanism at lower excitation levels. These are distinguished by their different dependences on the density of free carriers generated by the pump pulse. We are thereby able to determine a demarcation free-carrier density between these two optical-excitation regimes in which different physical processes dominate the relaxation of optically induced reflectivity and transmission changes. Studies of materials with different densities of deep band-tail states confirm the expected dependence of the demarcation free-carrier density on the trapping properties of the amorphous material; i.e., in a material with a higher density of deep band-tail states, a higher pump power is required before the ultrafast process becomes observable.

### II. EXPERIMENTAL PROCEDURES

Time-resolved reflectivity data were obtained in a conventional pump-probe geometry with a stepper-motor-driven delay stage. The pump and probe beams at 2 eV (625 nm) were orthogonally polarized and focused onto the sample using two different lenses giving a pump-to-

probe spot radius ratio of approximately 4:1. The probe beam was further attenuated to give a maximum fluence ratio between pump and probe beam of approximately 10:1. The fluence was determined by measuring the transmission through calibrated pinholes. In order to separate trapping processes from recombination processes, the excitation level was varied by several orders of magnitude. To cover the fluence regime between about 0.6 and 15 mJ/cm<sup>2</sup>, pulses from a colliding-pulse mode-locking (CPM) laser were amplified in a copper-vapor laser-pumped multipass amplifier,<sup>9</sup> and then used as the pump and probe beams, respectively. The pulse duration was about 50 fs with a total energy after amplification of a few  $\mu$ J per pulse and a repetition rate of approximately 7 kHz. For the low fluence regime between 10 and 100  $\mu$ J/cm<sup>2</sup>, a cavity-dumper-driven CPM system operating at 800 kHz (FWHM=80 fs) was used. Details on data acquisition and processing are discussed elsewhere.<sup>10</sup>

The amorphous silicon films used in this study have been prepared by reactive magnetron sputtering (RMS) of silicon in a hydrogen atmosphere. Details concerning the method of preparation have been published elsewhere.<sup>11</sup> In this paper, we will discuss two types of thin film material: *device quality a-Si:H*, with an optimum hydrogen content of about 5–10 at %, and *nonhydrogenated a-Si*, with a substantially higher density of band-tail traps. Both types of material were deposited onto both fused silica and crystalline silicon (*c-Si*) substrates. Relevant optical data for these samples are given in Table I. The partial Fresnel coefficients *a* and *b* are defined by

$$\frac{\Delta R}{R_0} = a(\Delta\epsilon_1) + b(\Delta\epsilon_2), \quad (1)$$

where  $\Delta\epsilon_1$  and  $\Delta\epsilon_2$  are the real and imaginary parts, respectively, of the complex dielectric function  $\epsilon_c = \epsilon_1 + i\epsilon_2$ .

### III. EXPERIMENTAL RESULTS AND DATA REDUCTION

Simultaneous reflectivity and transmission measurements have been performed on the thin-film *a-Si:H* and *a-Si* samples deposited onto the fused-silica substrates. In these films, the reflectivity and transmission changes are modified by multiple interferences within the highly absorbing film and the transparent substrate. Time-resolved reflectivity measurements have been performed

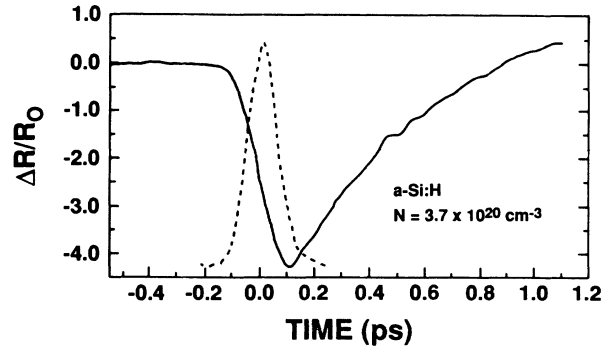


FIG. 1. Transient reflectivity measured on an *a-Si:H* film after high-level optical excitation. The cross-correlation function of pump and probe beam are also shown.

for comparison on the thin-film samples deposited on *c-Si*. They are free of multiple interferences, and the transient changes of reflectivity can be directly related to changes of the refractive index  $\Delta n$  at the surface of the irradiated film.

In Fig. 1, the reflectivity induced in an *a-Si:H* film deposited on a *c-Si* substrate is shown on a subpicosecond time scale. The cross correlation of the pump and probe beam, measured by two-phonon absorption in GaP, is shown as an inset. During the duration of the excitation pulse, the reflectivity is observed to initially decrease. This negative-going change reaches a maximum at the end of the pulse, recovers to the unperturbed-value reference level of the reflectivity within one picosecond, and then becomes positive going for longer time delays. Since the band gap in both of the amorphous silicon materials is smaller than the energy of the exciting laser beam, 2 eV, photogenerated carriers are excited into extended states. This type of reflectivity signature, which has also been observed for the nonhydrogenated *a-Si*, can then be attributed to a modification of refractive index by free hole-electron pairs whose density, as a function of time after the excitation pulse, is controlled either by a recombination or trapping process. An initial negative-going signal is a result of the experimental conditions in which the optical properties of the amorphous materials are being probed at a photon energy that is greater than the plasma frequency of the photogenerated free carriers.

TABLE I. Optical properties of the amorphous Si films.

Sample	Film thickness (nm)	Absorption constant <i>K</i>	Refractive index <i>n</i>	Thermo-optic coeff. $\partial(K^{-1})$	Band gap (Ref. 12) <i>E<sub>g</sub></i> (eV)	Partial Fresnel coefficients	
						<i>a</i>	<i>b</i>
<i>a-Si:H</i>	2400 (on Si)	0.2	3.44	$5.1 \times 10^{-4}$	1.73	0.0248	0.485
	1200 (on silica)						
<i>a-Si</i>	1200 (on Si)	0.6	4.4	$8 \times 10^{-4}$	1.5	0.0148	0.146
	240 (on silica)						

Above the plasma frequency, the reflectivity increases with increasing energy, therefore an increase in the carrier density increases the plasma frequency which leads to a reduction in the reflectivity.

The absorption induced in an *a*-Si:H film deposited on fused silica is shown in Fig. 2 together with the cross correlation of pump and probe beams. The change in the absorption constant  $\Delta k$  has been determined from simultaneous measurements of the reflectivity and the transmission. During the optical-excitation process, the induced absorption rises and reaches a maximum at the end of the pulse. After the end of the excitation pulse,  $\Delta k$  starts to recover, but only slowly, and on a subpicosecond time scale. This recovery of  $\Delta k$  is much slower than the recovery of the reflectivity (or  $\Delta n$ ) at a comparable excitation density. Fauchet *et al.* have attributed this behavior in  $\Delta k$  to a positive contribution to induced absorption, caused by lattice heating.<sup>5</sup> Similarly, the recovery of the negative-induced reflectivity change is faster due to a positive thermo-optical contribution. Since the maximum increase of the induced absorption is correlated with the integral of the exciting pulse, rather than to the pulse height, we can exclude the contribution of higher-order absorption processes. Therefore, the density of induced carriers  $N$  is simply proportional to the absorbed fluence. Based on the partial Fresnel coefficients, the contribution of the induced absorption  $\Delta k$  to the change of reflectivity  $\Delta R$  at the surface of the irradiated film is small ( $< 5\%$  of  $\Delta R$ ).

The maximum negative change of bulk reflectivity reached immediately after the generation of free electron-hole pairs scales linearly with the absorbed fluence  $F\alpha(1-R)$ , of the density of carriers created  $N$ , as shown in Fig. 3;  $F$  is the incident photon flux and  $\alpha$  is the absorption constant. The slope in Fig. 3,  $(\Delta R/R_0)/[F\alpha(1-R)]$ , however, depends on the properties of the amorphous silicon materials; e.g., the optical band gaps of *a*-Si:H and *a*-Si, etc.<sup>12</sup> The relevant optical properties are tabulated in Table I. To obtain quantitative information on the magnitudes of the dielectric constant changes  $\Delta\epsilon_1$  and  $\Delta\epsilon_2$ , we apply the well-known Drude relationships:

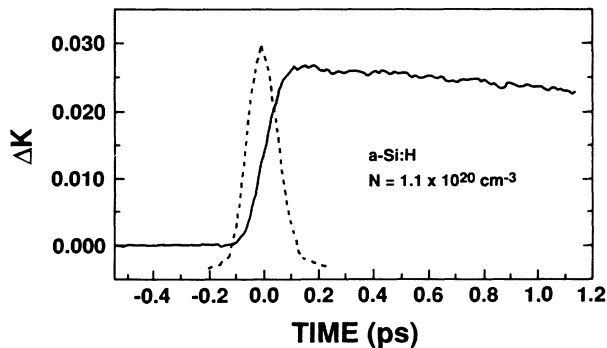


FIG. 2. Transient absorption in an *a*-Si:H film calculated from simultaneous reflectivity and transmission measurements.

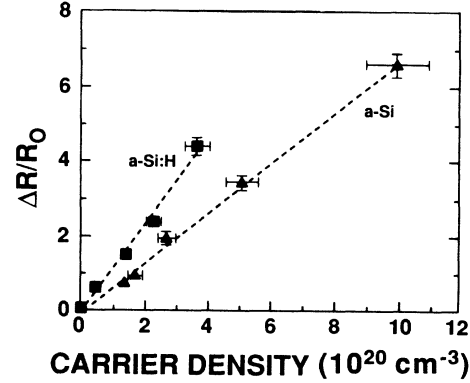


FIG. 3. Absolute value of the maximum induced reflectivity change  $\Delta R$  as a function of the absorbed fluence.

$$\Delta\epsilon_1 = \frac{-Ne^2}{m^* \epsilon_0 (\omega^2 + \tau_d^{-2})}, \quad (2)$$

$$\Delta\epsilon_2 = \frac{-\Delta\epsilon_1}{\omega \tau_d}, \quad (3)$$

where  $m^*$  is the optical reduced mass, and  $\tau_d$  the Drude damping time.  $\epsilon_0$  is the optical frequency dielectric constant of the amorphous semiconductor material, assumed to be constant in the energy regime in which the spectroscopy studies are performed, and  $(Ne^2/m^* \epsilon_0)^{1/2}$  is the plasma frequency of the photogenerated free carriers.

Drude damping times  $\tau_d$  have been determined for *a*-Si:H ( $\tau_d = 0.8$  fs) and *a*-Si ( $\tau_d = 0.5$  fs) from the simultaneous reflectivity and transmission measurements, and by the application of Eq. (3). To determine  $\tau_d$ ,  $\Delta k$  and  $\Delta n$  were evaluated from simultaneous measurements of  $\Delta T$  and  $\Delta R$  on amorphous films deposited on fused silica. Since the variation of  $k$  due to a plasma is related by  $\Delta k = -\Delta n / \omega \tau_d$ , this relation can be used to directly calculate the Drude damping time  $\tau_d$ . The specific change in reflectivity for each of these materials is given by Eq. (1), with the partial Fresnel coefficients  $a$  and  $b$  given in Table I. Using Eqs. (1) and (2), we obtain optical reduced masses of  $m^* = 0.12m_0$  for *a*-Si:H and  $m^* = 0.09m_0$  for *a*-Si. The band-averaged mobility effective masses for electrons and holes in *c*-Si are  $0.26m_0$  and  $0.36m_0$ , and when combined they yield an ambipolar (or reduced) effective mass of  $0.15m_0$ .<sup>13</sup> The optical reduced masses we obtain from the analysis of the amorphous-silicon data are comparable to the ambipolar mass for crystalline silicon, and therefore indicate that the properties of free carriers well removed from band-tail trapping states are very similar to the crystalline material.

Figure 4(a) shows the transient reflectivity measured on an *a*-Si:H film deposited on a *c*-Si substrate for three different levels of optical excitation that give rise to free-carrier densities  $N$  ranging from  $4.0 \times 10^{18}$  to  $3.7 \times 10^{20} \text{ cm}^{-3}$ . We note that as the excitation level increases, the initial (and also the fast) component for the free-carrier relaxation  $\tau$  also becomes faster, i.e., that  $\tau$  decreases as  $N$  increases. This same type of behavior for the initial fast component of the relaxation is observed for *a*-Si, de-

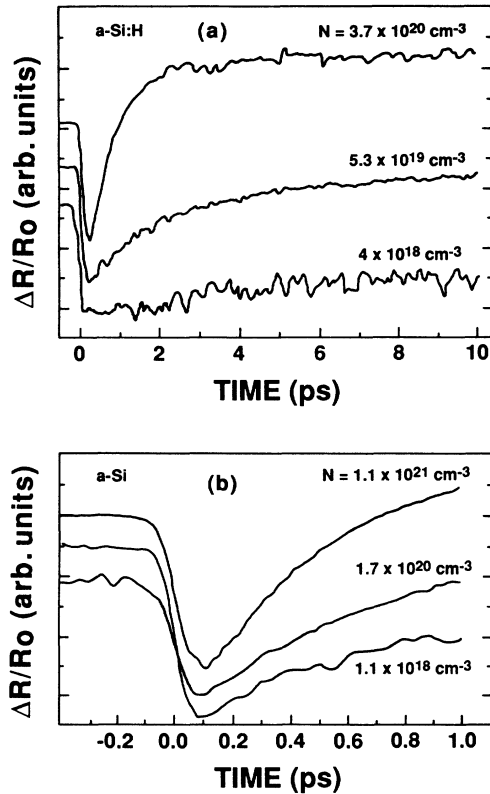


FIG. 4. Time-resolved reflectivity changes in (a) *a*-Si:H and (b) *a*-Si at different free-carrier densities. The initial recovery becomes faster with increasing free-carrier density. For better comparison the plots have normalized amplitudes.

positioned on *c*-Si, as is shown in Fig. 4(b). [Note the change in time scales between Figs. 4(a) and 4(b)]. In Fig. 5, the initial recovery time  $\tau$  is plotted versus  $N$ , the density of optically excited free carriers, both on logarithmic scales. For both materials, we can clearly identify two different regimes of behavior for  $\tau$  as a function of  $N$ . For high excitation levels ( $N > 5 \times 10^{18} \text{ cm}^{-3}$  for *a*-Si:H and

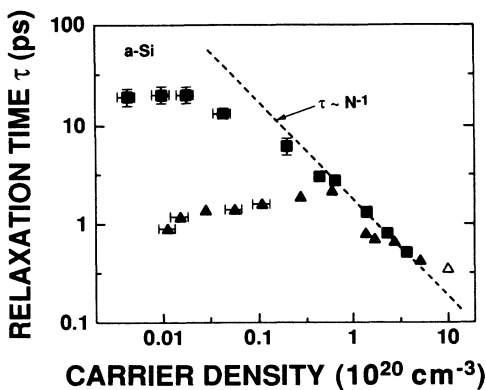


FIG. 5. Initial recovery time  $\tau$  of the reflectivity changes versus the photogenerated free-carrier density. The initial recovery time is taken to be the time it takes the reflectivity to recover fully. This is determined by extrapolation of the initial recovery slope, which is determined immediately after the excitation has finished.

$N > 8 \times 10^{19} \text{ cm}^{-3}$  for *a*-Si), we find an inverse linear dependence of  $\tau$  on the carrier density for both materials. In the hydrogenated material, the time constants level off to a value of  $\tau = 25 \text{ ps}$  at carrier densities below  $5 \times 10^{18} \text{ cm}^{-3}$ . In contrast, in the nonhydrogenated material,  $\tau$  reaches a maximum value of 2 ps at about  $10^{20} \text{ cm}^{-3}$  and then decreases below this excitation density.

The time decay of the reflectivity change is closely correlated to the removal or elimination of free carriers, which can occur either by recombination of *e-h* pairs, or by trapping of either carrier into localized states. For the high-density regime, we have observed a reciprocal dependence on injected carrier density for the initial decay of reflectivity. In terms of recombination processes, this behavior corresponds to a quadratic relationship:

$$\frac{dN}{dt} = \gamma N^2. \quad (4)$$

From Fig. 5, we determine approximately the same recombination coefficient for *a*-Si:H and *a*-Si. This parameter is then independent of the microstructure and the density of localized states, which are known to be very different in hydrogenated and nonhydrogenated amorphous silicon.

#### IV. DATA ANALYSIS

The experimental data shows that for high excitation conditions a quadratic recombination process determines the transient change of reflectivity. The rate equations can now be applied to determine both the free-carrier density and the lattice temperature  $T$  as functions of time. These equations were solved numerically using finite-difference procedures. To calculate the rate of quadratic recombination, we use  $\gamma = 7 \times 10^{-9} \text{ cm}^3 \text{ s}^{-1}$  for *a*-Si:H, and a slightly smaller value  $\gamma = 5 \times 10^{-9} \text{ cm}^3 \text{ s}^{-1}$  for *a*-Si. Equations (2) and (3) were used to calculate the change of the optical-frequency dielectric functions associated with changes in free-carrier plasma density. To account for changes in the dielectric functions that result from changes in the lattice temperature, we use  $dn = \vartheta \times dT$ , where  $\vartheta$  is the thermo-optical coefficient, and  $n$  is the index of refraction.  $\vartheta$  is then given by

$$\vartheta = \frac{dn}{dT} = \frac{-(n^2 + 1) \bar{E}_g}{n(E_g^2 - \hbar^2 \omega^2) dT}, \quad (5)$$

where we have set  $dE_g/dT = 3.6 \times 10^{-4} \text{ eV/K}$  for both *a*-Si and *a*-Si:H,<sup>14</sup> and for the average bandgap  $\bar{E}_g$  we have set  $\bar{E}_g = 3.7 \text{ eV}$  for *a*-Si:H and  $\bar{E}_g = 3.3 \text{ eV}$  for *a*-Si.<sup>15</sup> The excellent agreement between calculated and measured reflectivities as functions of time is demonstrated in Figs. 6(a) and 6(b). The fact that the fit reproduces the entire positive-going thermo-optic contribution to reflectivity can be taken as evidence for a nonradiative process.<sup>16</sup> The results also indicate that the quadratic recombination law holds for the entire time scale of observation in our experiments. For the comparisons given in Figs. 6(a) and 6(b) we used values of  $\vartheta$  calculated from Eq. (5). We have also measured directly by determining the change in the same reflectivity as a function of temperature. The values of  $\vartheta$  obtained in this way are lower

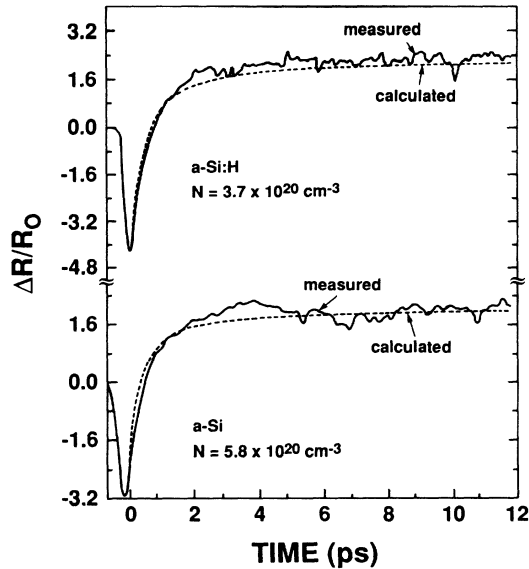


FIG. 6. Comparison between measured and calculated reflectivity data for (a) *a*-Si, and (b) *a*-Si:H, both as deposited on *c*-Si substrates.

by about  $30 \pm 10\%$  than the calculated values of  $\vartheta$ . These differences, however, do not change our conclusions relative to the evidence for a nonradiative recombination process.

From the discussion given above, we conclude that at high excitation levels there is a bimolecular nonradiative recombination process that dominates the free-carrier relaxation. The experimental data that we obtain are consistent with an Auger recombination mechanism that involves spatially correlated *e-h* pairs. An Auger recombination mechanism of this type has previously been proposed to explain the recombination of correlated *e-h* pairs in time-resolved luminescence measurements at high optical-excitation levels.<sup>8</sup> The Auger process, which is usually of third order in  $N$ ,<sup>17</sup> can become a second-order process if the electrons and holes are correlated as spatially overlapping pairs.<sup>5</sup> In this modified process, a recombining *e-h* pair transfers its energy to a neighboring pair, and the neighboring pair then dissociates and dissipates the excess kinetic energy by phonon emission, all on an ultrafast time scale. These processes start as soon as *e-h* pairs with correlated electron-hole wave functions are generated in extended states and have spatial overlap with the wave functions of other photogenerated *e-h* pairs. We then propose that an Auger recombination mechanism determines the recovery of the induced refractive-index change, and that this process starts immediately after the optical excitation of *e-h* pairs into extended states. The recombination coefficient  $\gamma$  for the ultrafast recombination process has been found to be approximately the same for both *a*-Si:H and *a*-Si. Since the thin-film microstructure, and the resulting density of localized states are very different for these two materials, recombination from localized states cannot explain the ultrafast reflectivity decay at these high excitation levels.

This lends additional support to the Auger mechanism which involves *e-h* pairs in the extended states.

The different band-tail structures of *a*-Si and *a*-Si:H become important only at lower optical-excitation densities. Since the recombination slows down with decreasing density, other relaxation processes can become observable below a demarcation density of optical excitation. In *a*-Si:H this demarcation density of about  $3-6 \times 10^{18} \text{ cm}^{-3}$  is at least ten times smaller than in the nonhydrogenated *a*-Si (see Fig. 5) which is known to have a higher density of defect states and band-tail states. We therefore conclude that this demarcation density is governed by trapping of carriers from extended states into localized band-tail states or defect states. In *a*-Si:H the density of deep-defect states ( $10^{16} \text{ cm}^{-3}$ ) is much smaller than the optically induced densities,<sup>18</sup> so that any contributions to the initial relaxation processes due to deep trapping can be neglected. The density of localized states close to the mobility edge is at least  $10^{20} \text{ cm}^{-3}$ . To obtain this value, we have assumed the usual exponential form for the density of band tail states [ $N_{BG} = N_C \exp(-E/E_0)$ ]. The zero of energy is at the mobility edge, and according to Street, we used  $N_C = 4 \times 10^{21} \text{ cm}^{-3}/\text{eV}$ .<sup>19</sup> With the commonly used  $E_0 = 30 \text{ meV}$  we calculate  $N_{BG} = 1.2 \times 10^{20} \text{ cm}^{-3}$  for the total density of states in the band tail. These localized states will then play a role in the relaxation processes in the low-excitation regime. Thus the observed initial relaxation at lower densities can be ascribed to trapping in shallow band-tail states. The large number of shallow states cannot be saturated in the low-excitation regime, explaining the observed density independence of  $\tau$  (Fig. 5), i.e.,  $\tau$  is not a function of  $N$ .

In this low optical-excitation-density regime, relaxation is much faster in *a*-Si than in the hydrogenated material (*a*-Si:H) due to a higher density of band-tail states and defect states. Since the density of band-tail states in *a*-Si is on the order of  $10^{21} \text{ cm}^{-3}$ ,<sup>20</sup> these states cannot be saturated by the trapping of optically induced carriers in the low-excitation regime. Nevertheless, we observe an increase of  $\tau$  with increasing carrier density (see Fig. 5), indicating some saturation of traps for the more highly defective, nonhydrogenated material. We speculate that this behavior may indicate the saturation of a subset of deep trapping states, e.g., those associated to dangling bonds. For this to be the case, those states would have to have a density of about  $5 \times 10^{19} \text{ cm}^{-3}$ ,<sup>18</sup> which is still significantly lower than the band-tail density.

## V. CONCLUSIONS

We have shown that the time-dependent optical response of *a*-Si:H and *a*-Si can be fully described by an optical model including the Drude-type response of a free-carrier plasma and a thermo-optical contribution to account for changes in lattice temperature. A demarcation carrier density has been identified for each material separating two different regimes for free-carrier relaxation. Above this demarcation free-carrier density the free-carrier density is controlled by a bimolecular nonradiative recombination mechanism, interpreted by us as

Auger recombination of spatially overlapping  $e-h$  pairs. This interpretation is consistent with the arguments developed in Refs. 7 and 8 for similar processes observed in photoluminescence for high optical pumping conditions. For densities less than the demarcation density, the free-carrier density is controlled by trapping into localized band-tail states. The demarcation density at which the relaxation mechanism changes from a bimolecular nonradiative (Auger) process to trapping is governed by the density of localized states in the amorphous sil-

icon, which depends on materials parameters such as the degree of hydrogenation.

#### ACKNOWLEDGMENTS

This work has been supported through funding from the North Carolina Board of Science Technology, the state of Nordrhein-Westphalen, and the Office of Naval Research.

- 
- <sup>1</sup>Z. Vardeny, C. Thomson, and J. Tauc, *Appl. Phys. Lett.* **42**, 580 (1983).
- <sup>2</sup>Z. Vardeny and J. Tauc, in *Disordered Semiconductors*, edited by M. A. Kastner *et al.* (Plenum, New York, 1987), p. 339.
- <sup>3</sup>J. Kuhl, E. O. Gobel, Th. Pfeifer, and A. Jonietz, *Appl. Phys. A* **34**, 105 (1984).
- <sup>4</sup>P. M. Fauchet, D. Hulin, A. Migus, A. Antonetti, J. Kolodzey, and S. Wagner, *Phys. Rev. Lett.* **57**, 2438 (1986).
- <sup>5</sup>C. Tanguy, D. Hulin, A. Mourchid, P. M. Fauchet, and S. Wagner, *Appl. Phys. Lett.* **53**, 880 (1988).
- <sup>6</sup>G. Noll and E. O. Gobel, *J. Non-Cryst. Solids* **97&98**, 141 (1987).
- <sup>7</sup>W. Rehm and R. Fischer, *Phys. Status Solidi B* **94**, 595 (1979).
- <sup>8</sup>R. A. Street, *Phys. Rev. B* **23**, 861 (1981).
- <sup>9</sup>W. M. Knox, M. C. Downer, R. L. Fork, and C. V. Shank, *Opt. Lett.* **9**, 552 (1984).
- <sup>10</sup>W. Kutt, K. Seibert, A. Esser, U. Lemmer, A. M. Malvezzi, and H. Kurz (unpublished).
- <sup>11</sup>R. A. Rudder, J. W. Cook, Jr., and G. Lucovsky, *Appl. Phys. Lett.* **45**, 887 (1984).
- <sup>12</sup>G. N. Parsons and C. Wang (unpublished).
- <sup>13</sup>S. Wang, *Solid State Electronics* (McGraw-Hill, New York, 1966), Chaps. 3, 4, and 5.
- <sup>14</sup>G. D. Cody, B. Abeles, C. R. Wronsky, B. Brooks, and W. A. Lanford, *J. Non-Cryst. Solids* **35&36**, 463 (1980).
- <sup>15</sup>L. Ley, in *The Physics of Hydrogenated Amorphous Silicon*, Vol. 56 of *Topics in Appl. Physics*, edited by J. D. Joannopoulos and G. Lucovsky (Springer, Berlin, 1984), Chap. 3.
- <sup>16</sup>M. C. Downer and C. V. Shank, *Phys. Rev. Lett.* **56**, 761 (1986).
- <sup>17</sup>N. G. Nilson, *Phys. Scr.* **8**, 165 (1973).
- <sup>18</sup>M. H. Brodsky, in *Fundamental Physics of Amorphous Semiconductors*, Vol. 25 of *Springer Series in Solid-States Sciences* (Springer-Verlag, Berlin, 1981).
- <sup>19</sup>R. A. Street, *SPIE*, Vol. 763, 11, *Physics of Amorphous Semiconductors Devices* (1987).
- <sup>20</sup>R. A. Street and D. K. Biegelsen, in *The Physics of Hydrogenated Amorphous Silicon*, Vol. 56 of *Topics in Applied Physics*, edited by J. D. Joannopoulos and G. Lucovsky (Springer, Berlin, 1984), Chap. 5.